

# Numerical Investigation of the In-Plane Shear Behaviour of Aligned Discontinuous Fibre Composites under Processing Conditions

Hao Yuan<sup>1,a\*</sup>, Burak Ogun Yavuz<sup>1,b</sup>, Yuncong Feng<sup>1,c</sup>, Ian Hamerton<sup>1,d</sup>,  
Byung Chul Kim<sup>1,e</sup>, Stephen R. Hallett<sup>1,f</sup> and Jonathan P.-H. Belnoue<sup>1,g</sup>

<sup>1</sup>Bristol Composite Institutes, University of Bristol, Bristol BS8 1TR, United Kingdom

<sup>a</sup>Hao.Yuan@bristol.ac.uk, <sup>b</sup>Ogun.Yavuz@bristol.ac.uk, <sup>c</sup>ol24008@bristol.ac.uk,  
<sup>d</sup>Ian.Hamerton@bristol.ac.uk, <sup>e</sup>B.C.Eric.Kim@bristol.ac.uk, <sup>f</sup>Stephen.Hallett@bristol.ac.uk,  
<sup>g</sup>Jonathan.Belnoue@bristol.ac.uk

\*corresponding author

**Keywords:** aligned discontinuous fibres, forming simulation, in-plane shear.

**Abstract.** Aligned discontinuous fibre reinforced composites (ADFRC) have demonstrated an improved formability for small to medium sized parts with complex geometries compared to the continuous fibre based prepreg due to their stretchability along the fibre direction. The process simulation tool developed for this class of materials so far mostly concerns their tensile behaviour along the fibre direction. However, neglecting other deformation modes like the in-plane shear in a forming simulation may pose risks for the correct prediction of formed shape. This study verified a strategy which adopts previously developed analytical micromechanical models for tensile and in-plane shear deformation of ADFRCs, in a finite element framework. The implementation is validated by comparing results from virtual shear tests against experiments at different temperatures. This was then followed by virtual forming experiments on a doubly curved geometry, in which the tensile and shear properties of the material were varied separately to study the effects of each deformation mechanism on the simulated forming behaviour of the material.

## Introduction

Highly aligned discontinuous fibre reinforced composites (ADFRC) manufactured using High-Performance Discontinuous Fibre (HiPerDiF) technology [1], originated from University of Bristol, have been shown to retain the mechanical properties comparable to those of continuous fibre-based counterparts when their fibres are longer than critical length and aligned well in the loading direction. Additionally, the possible movement between discontinuous fibres during forming helps reduce the process-induced defects like wrinkling, which enhances the deformability in the forming of complex 3D shapes [2]. Beyond these processing advantages, a notable feature of these materials is their capability to repurpose reclaimed carbon fibres, thereby supporting the circular-economy and reducing the environmental burden associated with composite manufacturing. Coupled with fast snap-cure resin systems, ADFRC prepreps represent promising candidates for high-rate production of lightweight structural components. These developments underscore the need for reliable simulation frameworks capable of predicting deformation behaviour and process-induced defects to guide material and process optimisation at scale.

There have been attempts made to assess the formability of ADFRCs through quantitative experimental studies at specimen [3] and preform levels [4]. However, these approaches only consider the tensile deformation along fibre direction and obtained experimental results are material and layout specific, meaning that new test campaigns are required for different ADFRC materials. Over the past two decades, forming simulation for continuous fibre-based composites has matured and the simulation frameworks for textile composites typically adopt in-plane shear and out-of-plane bending as key input parameters to predict forming behaviour and major defects like wrinkling [5,6]. More recently, the community has begun to adapt these constitutive approaches to highly aligned discontinuous fibre composites [7,8], focussing primarily on their ability to deform along the fibre direction. However, this emphasis risks overlooking the influence of other deformation mechanisms.

In particular, the role of in-plane shear in aligned discontinuous fibre preregs remains underexplored and inaccurate representation of shear properties may affect defect formation, post-forming shape and fibre orientation.

This study verified an analytical micromechanical model for in-plane shear behaviour of epoxy-based ADFRC preregs [9] and then investigated the effects of in-plane shear deformation on the forming behaviour through a series of virtual tests. In the finite element framework developed in [9], the analytical models which relate both tensile [7] and shear deformations of the ADFRC prepreg to shearing of the matrix and its rheological properties were integrated into a hypoelastic based constitutive model developed for forming of fibrous materials, which were implemented in ABAQUS/Explicit through VUMAT subroutine. While in [9] the matrix viscosity values were directly taken from the supplier's data sheet, rheological properties of the matrix materials investigated in current study were measured via the oscillatory rheology experiment at a range of temperature and shear rates. Furthermore, a ratio between experimentally measured in-plane tensile and out-of-plane bending properties was assigned to the hybrid membrane-shell elements to fully decouple material's in-plane and out-of-plane behaviours while correctly projecting the total stiffness. The shear test simulation was performed to verify the modelling approach for in-plane shear behaviour, and force-displacement results were compared against the experimental curves. The effects of in-plane shear properties on the forming behaviour of ADFRCs were studied using forming simulations with tensile and shear properties from different temperatures.

### Material Characterisation

The ADFRC investigated in this study was a unidirectional tape produced with HiPerDiF technology and made with 3 mm-long carbon fibres and polylactic acid (PLA) matrix. The same HiPerDiF tape has been used in a previous study on its tensile behaviour [7], where material properties of the fibre and matrices were given. In the previous study, the oscillatory rheology experiments were conducted for the PLA matrix material to obtain the viscosity  $\eta$  and storage modulus  $G$  based on the Maxwell model (Eq. 1) at different temperatures for both amorphous and semi-crystalline phases:

$$\tau + \eta \dot{\tau} / G = \eta \dot{\gamma}. \quad (1)$$

where  $\dot{\tau}$  and  $\dot{\gamma}$  are shear stress rate and shear strain rate in the matrix, respectively. In the more recent study [9], the obtained rheological properties of the matrix were also related to the shear behaviour of an epoxy-based tape in the modelling in addition to its tensile behaviour. The manufacture of the prepreg tape with HiPerDiF technology, was described in detail in [1]. The width and thickness of the manufactured tape are 5 mm and 1 mm, respectively. Fig. 1 shows the modified picture-frame test rig [10] used in this study with PLA-based HiPerDiF test specimens before and after the test. The same test procedure as demonstrated in [9] was followed for the PLA-based tape in current study. The tape was clamped on the test rig with fibres oriented in the horizontal direction. As shown in Fig. 1 (b), by pulling up the moving block on each side with the central block fixed, the effective in-plane shearing occurs symmetrically in two 10 mm  $\times$  5 mm regions. Due to the difficulty in reaching a uniform temperature distribution above 100°C, the test was performed only at 100°C and a shear strain rate of 0.001 rad/s, and the in-plane shear strain was measured using Stereo DIC with two 16MP cameras.

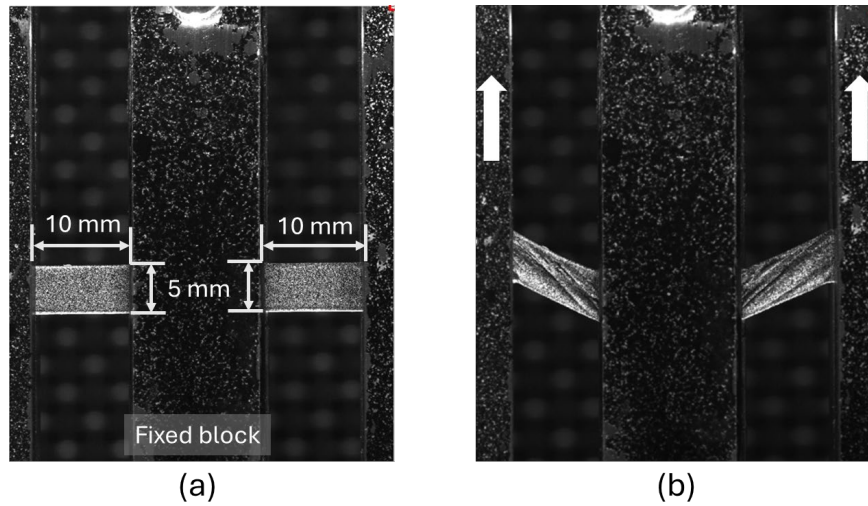


**Fig. 1.** Modified picture-frame test setup with PLA-based HiPerDiF test specimens (a) before the test and (b) after the test.

## Simulation

### Analytical models for tape deformation.

Due to the highly aligned fibres in ADFRCs, the microstructure evolution during loading of the composite tape can be idealised and the load developed in the composite tape is transferred through the matrix as shearing between aligned discontinuous fibres. The analytical micromechanical models for both tensile [7] and shear deformation [9] of ADFRCs developed by Yavuz et al. adopts the assumption above and relates the mechanical behaviour of the tape to its microstructures and rheological properties of the matrix. As demonstrated in [7], under tensile loading the shear strain rate of matrix material ( $\dot{\gamma}$ ) can be calculated from the strain rate of the tape in fibre direction ( $\dot{\varepsilon}_{11}$ ) as:

$$\dot{\gamma} = \dot{\varepsilon}_{11}(L - \delta)[K - 1]/D. \quad (2)$$

where  $L$ ,  $D$  and  $K$  are fibre length, fibre diameter and the geometric factor related to an assumed hexagonal fibre packing ( $K = 2.64$  [11]), respectively. After deriving the matrix shear stress ( $\tau$ ) from known rheological properties of matrix and matrix shear strain using Eq. 1, the change of stress in the tape along the fibre direction ( $\Delta\sigma_{11}$ ) can then be calculated from the shear stress change in matrix as:

$$\Delta\sigma_{11} = 2\Delta\tau f \delta / D. \quad (3)$$

where  $f$  is the fibre volume fraction of the uncured tape and  $\delta$  is the fibre overlap length calculated as a function of strain of the tape along the fibre direction:

$$\delta = (L/2)(a + b\varepsilon_{11} + c\varepsilon_{11}^2). \quad (4)$$

As proposed in [9], when the tape subject to in-plane shearing, the shear strain of matrix ( $\dot{\gamma}$ ) can be derived from the in-plane shear strain rate of the tape ( $\dot{\varepsilon}_{12}$ ) as follow with same geometric factor of fibre packing:

$$\dot{\gamma} = \dot{\varepsilon}_{12}K. \quad (5)$$

Following the derivation of matrix shear stress ( $\tau$ ) using Eq. 1, the change of in-plane shear stress of the tape ( $\Delta\sigma_{12}$ ) can then be calculated as:

$$\Delta\sigma_{12} = \Delta\tau. \quad (6)$$

### FE Implementation.

The numerical simulation of the shear test and a virtual double diaphragm forming was performed using Abaqus/Explicit following the similar strategy adopted in [7,9]. The HypoDrape VUMAT, a hypoelasticity-based user material subroutine specially developed for forming of thin fibrous materials [12], was modified to incorporate above analytical micromechanical models for tension and shear deformation of the HiPerDiF tape. The out-of-plane bending properties of the tape was decoupled from its in-plane material properties by the hybrid element consisting of membrane and shell elements sharing common nodes. Instead of applying in-plane properties in shell elements as in [9], the stiffness of shell elements in current study correlates to the bending stiffness of the tape only whereas the sum of the stiffness of shell and membrane elements represents the material tensile stiffness. Table 1 shows the material properties used for both element types for the PLA-based HiPerDiF tape. The analytical micromechanical model for tensile deformation was implemented for both element types for tensile properties along the fibre direction to account for effects of the tape deformation on its bending stiffness. Furthermore, cantilever bending test was performed using DMA (Dynamic Mechanical Analysis) for the material and ratios of its bending stiffness and tensile stiffness were measured as 0.48, 0.39, and 0.49 at 80°C, 100°C and 120°C, respectively [13]. The discrepancies of these values between different temperatures could be attributed to the variations from the experiment, including differences in strain rates between tensile and bending tests and crystallinity variations due to temperature inconsistencies. As shown in Table 1, these numbers were used as a multiplicative factor during the stress calculation for two types of elements.

**Table 1.** Material properties used for membrane and shell elements.

Element Type	Density [tonne/mm <sup>3</sup> ]	Fibre-Direction Properties [MPa]	Tensile	Transverse-Direction Tensile Properties [MPa]	Shear Properties [MPa]
Membrane	7.13E-05	Micromechanical model*(1-ratio)		0.1*(1-ratio)	Micromechanical model
Shell	7.13E-05	Micromechanical model*ratio		0.1*ratio	0

In the simulation of shear test, only effective shear region on the left was modelled due to symmetry of the rig. To replicate correct boundary conditions in the experiment, the right edge of the material was fixed while the left edge was constrained to a reference point which was connected to another fixed reference point on the right with a rigid link so that one can rotate around another when a vertical displacement is applied. It is worth noting that during experiments at high temperatures there was noticeable tensile deformation in the rig when the test machine pulling up the moving block, resulting in a smaller displacement of the moving edge than prescribed in the testing programme. Therefore, the displacement history obtained from the DIC was used in the simulation of shear tests. As multiple deformation modes (i.e. out-of-plane bending and tension) can be induced during the test in addition to in-plane shear due to buckling and alignment of the material edge and rig's rotation pins, force-displacement results were used to verify the model instead of the shear stress-strain results. Additionally, as shown in Fig. 2 a double diaphragm forming (DDF) process was also modelled to further investigate the effects of shear properties on the forming behaviour of the HiPerDiF preform. The simulation was set up in a similar way to that in [9], in which a two-ply preform ([0°/90°]) was placed between two diaphragm films under vacuum pressure and then formed over a doubly-curved mould by the vacuum between the bottom diaphragm and mould surface. Diaphragm films were stretched after pressure applied to both films to replicate the slight tension induced by the clamps in the real process.

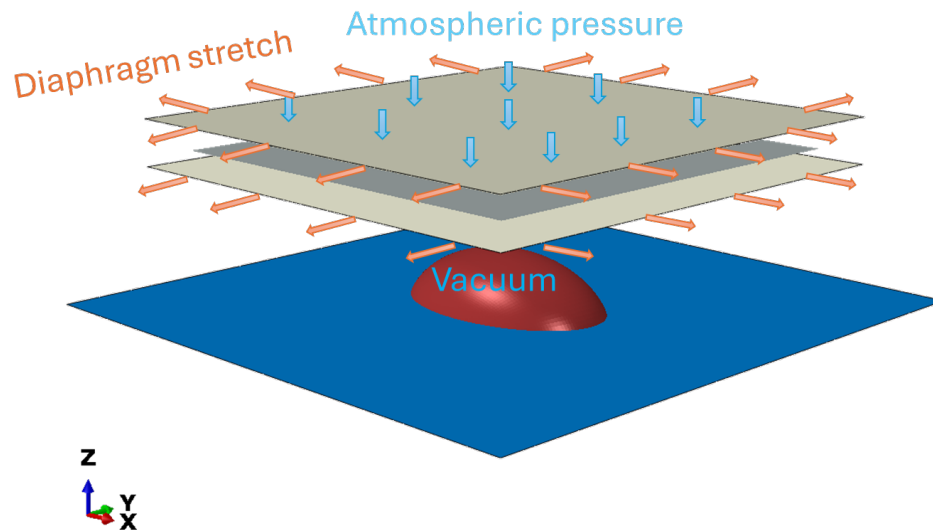
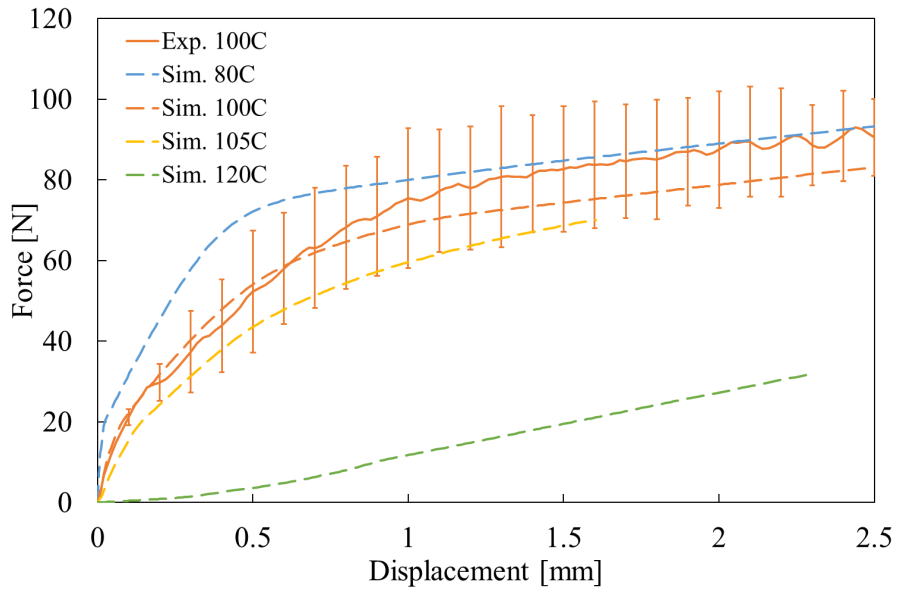


Fig. 2. Double diaphragm forming model setup and boundary conditions.

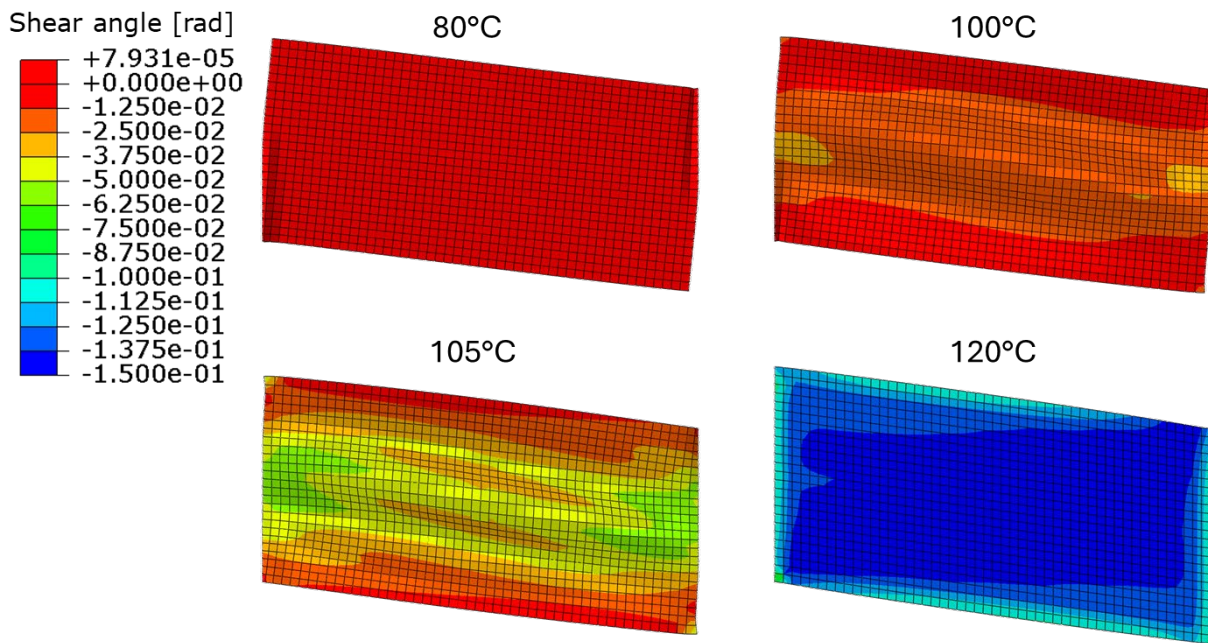
## Results and Discussion

Fig. 3 shows the averaged force-displacement curve from shear test at 100°C and simulation at four temperatures. Error bars on the experimental curve indicate the standard deviation from different test repeats. Note that the matrix rheologic properties at 105°C was interpolated from the rheology experiment results at 100°C and 120°C. The force-displacement from simulation at 100°C shows an overall good agreement with the experimental curve. For shear test simulation at 80°C, 100°C and 105°C, force-displacement curves have a similar characteristic shape with an initial sharp increase dominated by the in-plane shear deformation in the beginning of the test and a slower force increase at larger displacements related to the out-of-plane buckling and fibre direction tension induced by the rig. Additionally, the tension could also lead to potential sliding of the specimen edge within the clamps at larger displacement when tension becomes more prominent. These has led to much greater variations in the measured force after 0.5 mm displacement. However, significant effects of temperature can be seen between 105°C and 120°, at which only a slower increase of the force was observed. This was attributed to the reduction of resin properties, leading to overall lower mechanical properties of the specimen (e.g. tensile, shear and bending stiffness) and a different deformation behaviour during the test than that at lower temperatures.

This can be further analysed quantitatively through the shear angle distribution results in Fig. 4, which shows contours from shear test simulation at 1.5 mm crosshead displacement, corresponding to a theoretical shear strain of 0.15. It can be seen that the material's ability to shear improves with increased temperature and decreased matrix properties as the overall shear strain increases and its distribution becomes more uniform at higher temperatures. At 80°C, shearing the specimen is barely possible due to restricted relative sliding of fibres imposed by the "stiffer" matrix. As a result, rigid rotation of the specimen can occur, and severe buckling or tensile failure could appear at corners near the clamp due to high compression or tension in fibre direction. In contrast, the decreased tensile and bending stiffness and improved shearing capability lead to minimum wrinkling on the specimen at 120°C.



**Fig. 3.** Force-displacement results of experimental shear test at 100°C and numerical shear test simulation at 80°C, 100°C, 105°C and 120°C.



**Fig. 4.** Shear angle distribution (unit: rad) at 1.5 mm machine crosshead displacement for shear test specimens at four different temperatures.

As both tensile and shear deformations of the HiPerDiF prepreg are dominated by the shearing of matrix, it is difficult to study the effect or contribution of each individual deformation mode on the overall behaviour of the material. Therefore, in the virtual forming test the in-plane shear and tensile properties were decoupled in the VUMAT subroutine so that shear and tensile properties can be varied separately without affecting each other. As shown in Fig. 5 (a) and (d), forming simulations with real tension and shear properties were performed at 100°C and 120°C whereas Fig. (b) and (c) show the simulation with artificial properties (i.e. shear and tension responses use matrix rheological properties at different temperatures). The colour contour shows the ratio of thickness reduction of the preform  $\Delta t/t_0$  calculated from the in-plane strains ( $\varepsilon_1$  and  $\varepsilon_2$ ) using Eq. (7):

$$\Delta t/t_0 = 1 - \exp(-(\varepsilon_1 + \varepsilon_2)). \quad (7)$$

It can be observed that the preform could not conform to the mould at 100°C as large wrinkling was formed in the diagonals, further stiffening the HiPerDiF preform. At 120°C the preform exhibited

an improved conformity and less thinning in the centre, however, there was the presence of small wrinkling around the tight radii between the doubly curved surface and flat surface. It is worth noting that forming of PLA-based prepreg is normally performed at 140°C and the results related to forming simulation are only analysed qualitatively in this study. Increasing the tensile properties by using matrix rheological properties at 100°C instead (Fig. 5 (c)) shows no noticeable influence on the overall forming behaviour whereas increasing shear properties (Fig. 5 (b)) modifies the conformity of the preform, which is closer to that in the forming simulation with real tensile and shear properties at 100°C. This suggests that the in-plane shear response dominates the forming behaviour for PLA-based HiPerDiF preform under current process conditions.

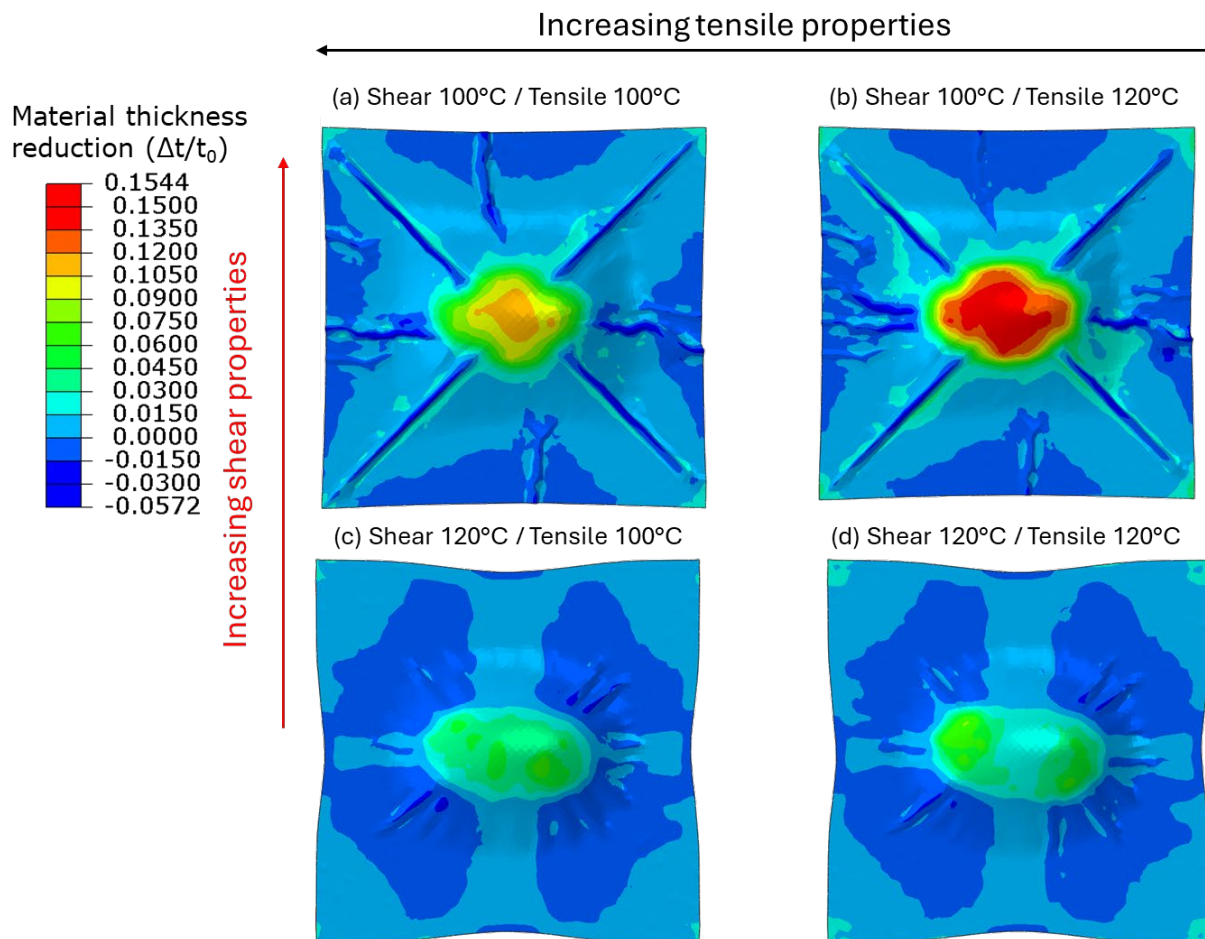


**Fig. 5.** Post-forming material thickness reduction ( $\Delta t/t_0$ ) for PLA-based HiPerDiF preform with different shear and tensile properties.

To further explore the influence of these deformation mechanisms, forming simulations were also performed for a HiPerDiF preform consisting of recycled carbon fibres and a snap-cure epoxy resin. Although directional tests (e.g. tensile and in-plane shear characterisation tests) have not been completed for this material, the deformation of this HiPerDiF material is still assumed to be dominated by the shearing of matrix when aligned discontinuous fibres slide against each other. Therefore, the same modelling strategy described in the previous section is followed to obtain the tensile and shear properties of the tape from its matrix rheological properties. Since rheological properties of the snap-cure epoxy are much lower than those of PLA and the deformation of ADFRC tape are dominated by the matrix properties, forming simulation was only performed at much lower temperature (i.e. 25°C and 40°C) for epoxy-based HiPerDiF preform to preserve the material integrity during the process. The same test procedure as in [7] was followed to obtain the storage modulus and viscosity values at varied shear rates for the epoxy resin at 25°C and 40°C. However, these values are not presented at this stage as further calibration is required once the test campaign is completed.

Similar to the forming simulations presented previously, two simulations with real shear and tensile properties and two simulations with artificial properties were performed for epoxy-based preform. Fig. 6 shows the results of four forming simulations with colour contours representing the thickness reduction of the preform. Compared to PLA-based preform, a much better conformity can be seen for the epoxy-based material as there was no noticeable wrinkling occurring for both simulations at 25°C and 40°C (Fig. 6 (a) and (d)). Nevertheless, the major concern on the defects here lies in thinning of the preform, as the reduction in thickness rises from 12% to above 22% when temperature increased from 25°C to 40°C. Increasing only shear properties did not change the resulted material thinning (Fig. 6 (b)) whereas increasing only tensile properties improved the result (Fig. 6 (c)), which is closer to that in a forming simulation at 25°C. This was attributed to the relatively lower apparent shear stiffness of the epoxy-based material compared to the PLA-based material (shear stresses observed in the preliminary simulations are in the order of  $\times 10^{-5}$  to  $\times 10^{-2}$  MPa), which was a result of the much lower matrix rheological properties. Due to high stretchability of the ADFRC prepreg, shear strain and shear strain rate of the matrix achieved through material tensile deformation in the fibre direction can be significantly greater than those achieved through shear deformation. Therefore, for this particular epoxy-based system, the increase in material tensile stiffness plays a much significant role in the change of forming behaviour than the increase in its apparent shear stiffness.

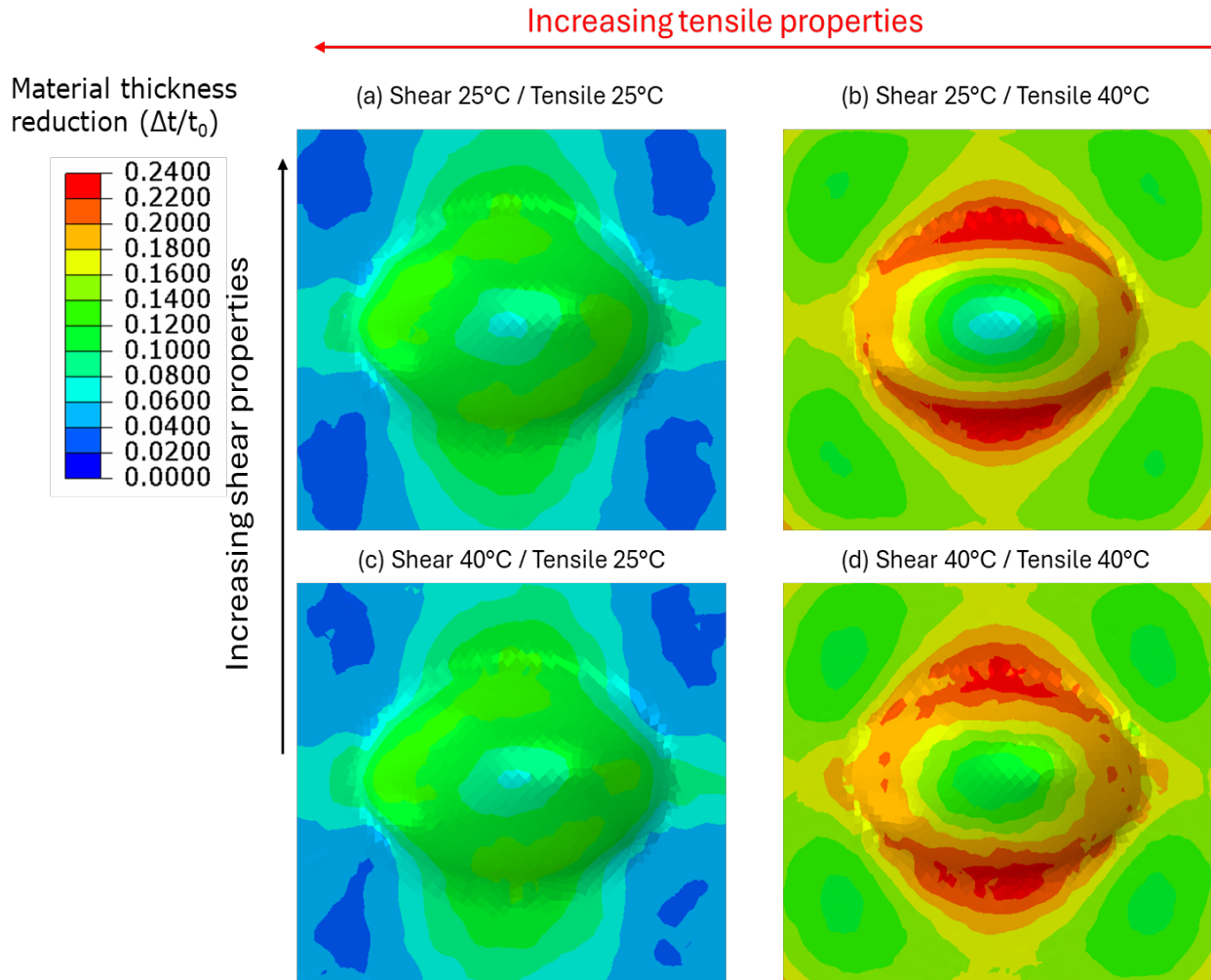


**Fig. 6.** Post-forming material thickness reduction ( $\Delta t/t_0$ ) for epoxy-based HiPerDiF preform with different shear and tensile properties.

## Conclusion

In this study, the finite element modelling approach with an analytical micromechanical model developed previously for shear deformation of ADFRCs has been verified through experimental and numerical tests. The predicted force-displacement curve from simulation agrees well with the experimental ones at 100°C test temperature, demonstrating that the shear deformation of HiPerDiF tape is also dominated by the shearing of matrix material. Curves show an initial increase corresponding to the prominent in-plane shear deformation followed by a slower increase after out-of-plane buckling occurs. Shear test simulations at different temperatures suggest that increased temperature can improve the material's ability to shear and significantly reduce wrinkling during this type of tests through improved stretchability. The current approach allows the model to be validated, as different deformation mechanisms (i.e. in-plane shear, out-of-plane bending and tension) can be captured during the test. It must be noted, however, that the current approach is insufficient to extract the shear properties due to the early apparition of out-of-plane wrinkling. Therefore, it is still necessary to improve the shear test for this class of materials to promote pure in-plane shear deformations for a range of relevant process conditions while maintaining the material integrity.

Forming simulations were performed for both PLA-based and epoxy-based HiPerDiF preforms to investigate the effects of in-plane shear and tensile properties on their overall forming behaviour. For each type of HiPerDiF material forming simulations were performed with real shear and tensile properties, and two simulations were performed with artificial properties where tensile and shear responses use matrix properties at different temperatures. The PLA-based preform showed a shear dominated forming behaviour with out-of-plane wrinkling as its major defects. In contrast, the epoxy-based preform demonstrated a tensile dominated forming behaviour due to relatively lower apparent material shear stiffness caused by low matrix rheological properties compared to PLA. With high stretchability of the material, the matrix shear achieved through material shear deformation can be much lower than that achieved through tension deformation, which further signifies the contribution of tensile properties in the overall deformation during forming for the epoxy-based preform. However, comparison with the results from ongoing experimental work is required to confirm these preliminary findings from the numerical study. Further analysis on the material deformation will also be performed to quantify the contribution of the in-plane shear properties on the forming behaviour of materials investigated.

This study highlights the importance of correct measurement of the matrix properties as well as an appropriate numerical tool that takes into account different deformation modes. Such a tool can be useful in virtual forming trials and help reduce the efforts on material tests if one of the deformation modes plays an insignificant role on the material's overall behaviour.

## Acknowledgement

This work was supported by the APC (Advanced Propulsion Centre UK)-funded SCALE-UP project (Sustainable Composite for Automotive and Low-Emission UK Production).

## References

- [1] H. Yu, K.D. Potter, M.R. Wisnom, A novel manufacturing method for aligned discontinuous fibre composites (High Performance-Discontinuous Fibre method), *Compos Part A Appl Sci Manuf* 65 (2014) 175–185.
- [2] T.A. Cender, P. Simacek, J.W. Gillespie, S.G. Advani, Microstructural evolution of highly aligned discontinuous fiber composites during longitudinal extension in forming, *Compos Sci Technol* 254 (2024).
- [3] L.J. Tomlin, T.A. Cender, S. Sauerbrunn, S.G. Advani, Methodology to establish a forming process window for thermoset aligned discontinuous fiber composites, *Compos Part A Appl Sci Manuf* 180 (2024).

- 
- [4] K.S. Morris, T.A. Cender, E.T. Thostenson, S. Yarlagadda, Forming limits of highly aligned discontinuous fiber composite laminates, *Compos Part A Appl Sci Manuf* 190 (2025) 108683.
- [5] P. Boisse, R. Akkerman, P. Carlone, L. Kärger, S. V. Lomov, J.A. Sherwood, Advances in composite forming through 25 years of ESAFORM, *International Journal of Material Forming* 15 (2022).
- [6] P. Harrison, Modelling the forming mechanics of engineering fabrics using a mutually constrained pantographic beam and membrane mesh, *Compos Part A Appl Sci Manuf* 81 (2016) 145–157.
- [7] B.O. Yavuz, I. Hamerton, M.L. Longana, J.P.-H. Belnoue, Modelling the tensile behaviour of aligned discontinuous carbon fibre thermoplastic matrix composites under processing conditions, *Compos Sci Technol* 269 (2025) 111252.
- [8] A. Stack, P. Simacek, A. Ford, K. Morris, T.A. Cender, S. Advani, Modeling the extension behavior of aligned discontinuous fiber prepreg during thermoforming, *International Journal of Material Forming* 18 (2025) 96.
- [9] T. Gordon, B.O. Yavuz, B. Zhang, X. Sun, I. Hamerton, M.L. Longana, S.R. Hallett, J.P.-H. Belnoue, B.C. Kim, Double-diaphragm forming of highly aligned short-fibre preforms for complex composite parts, *International Journal of Material Forming* 18 (2025) 85.
- [10] B. Zhang, B.C. Kim, Experimental characterisation of large in-plane shear behaviour of unidirectional carbon fibre/epoxy prepreg tapes for continuous tow shearing (CTS) process, *Compos Part A Appl Sci Manuf* 162 (2022).
- [11] R.B. Pipes, D.W. Coffin, P. Simacek, S.F. Shuler, R.K. Okine, Rheological Behavior of Collimated Fiber Thermoplastic Composite Materials, in: S.G. Advani (Eds.), *Flow and Rheology in Polymer Composites Manufacturing*, Elsevier Science B.V., Amsterdam, 1994, pp. 85-125.
- [12] A.J. Thompson, J.P.H. Belnoue, S.R. Hallett, Modelling defect formation in textiles during the double diaphragm forming process, *Compos B Eng* 202 (2020) 108357.
- [13] B.O. Yavuz, Forming simulations of aligned discontinuous fibre thermoplastic prepreg: towards right-first-time sustainable composite manufacturing, PhD thesis (2025), University of Bristol.